Incorporation of Fused Tetrathiafulvalenes (TTFs) into Polythiophene Architectures: Varying the Electroactive Dominance of the TTF Species in Hybrid Systems

Rory Berridge,[†] Peter J. Skabara,*[,†] Cristina Pozo-Gonzalo,[†] Alexander Kanibolotsky,[†] Jan Lohr,[†] Joseph J. W. McDouall,[†] Eric J. L. McInnes,[†] Joanna Wolowska,[†] Christoph Winder,[‡] N. Serdar Sariciftci,*[,‡] Ross W. Harrington,[§] and William Clegg[§]

School of Chemistry, University of Manchester, Oxford Road, Manchester M13 9PL, U.K., Linz Institute for Organic Solar Cells (LIOS), Physical Chemistry, Johannes Kepler University Linz, Linz A-4040, Austria, and School of Natural Sciences (Chemistry), University of Newcastle, Newcastle upon Tyne NE1 7RU, U.K.

Received: December 12, 2005

A novel polythienylenevinylene (PTV) and two new polythiophenes (PTs), featuring fused tetrathiafulvalene (TTF) units, have been prepared and characterized by ultraviolet−visible (UV−vis) and electron paramagnetic resonance (EPR) spectroelectrochemistry. All polymers undergo two sequential, reversible oxidation processes in solution. Structures in which the TTF species is directly linked to the polymer backbone (**2** and **4**) display redox behavior which is dictated by the fulvalene system. Once the TTF is spatially removed from the polymer chain by a nonconjugated link (polymer **3**), the electroactivity of both TTF and polythiophene moieties can be detected. Computational studies confirm the delocalization of charge over both electroactive centers (TTF and PT) and the existence of a triplet dication intermediate. PTV **4** has a low band gap (1.44 eV), is soluble in common organic solvents, and is stable under ambient conditions. Organic solar cells of polymer **4**:[6,6]-phenyl-C_{61} butyric acid methyl ester (PCBM) have been fabricated. Under illumination, a photovoltaic effect is observed with a power conversion efficiency of 0.13% under AM1.5 solar simulated light. The onset of photocurrent at 850 nm is consistent with the onset of the $\pi-\pi$ absorption band of the polymer. Remarkably, UV−vis spectroelectrochemistry of polymer **4** reveals that the conjugated polymer chain remains unchanged during the oxidation of the polymer.

Introduction

The design and synthesis of novel conjugated oligomer and polymer architectures continues to attract great attention in the field of organic semiconductors. The most critical advances focus on improved properties toward specific device applications, such as high mobilities for field effect transistors (OFETs),[1−4] high values of luminescence efficiencies for organic light emitting diodes (OLEDs),[5−7] control of absorption wavelength for OLEDs and electrochromic materials,[8−11] as well as low band gaps[12−17] and charge separation of excited states for organic photovoltaics.[18−20]

Organic conjugated oligomers and polymers exhibit semiconducting behavior and photo/electroactivity in the main chain of the materials. In this respect, the incorporation of secondary redox-active units into conjugated structures is a quandary. Does the additional electroactive species impart its electroactive character into a hybrid state, or does it simply act independently? There are several examples of conjugated materials that feature electroactive units tethered to the polymer backbone, and these include polythiophenes with ferrocene,[21] phthalocyanine,[22] transition metal complexes,[23] viologens,[24,25] fullerenes,[26,27] and anthraquinones.[28,29] Our own interests in this area are based on polythiophene−tetrathiafulvalene (TTF) hybrid materials. Although several groups have succeeded in attaching TTFs to polythiophene,[30−33] the fulvalene units are held by nonconjugated links, which render the TTFs electroactively independent. In a recent paper,[34] we presented the synthesis and properties of a thieno-TTF polymer in which the two heterocyclic units are fused together (**1**). In this work, we have shown that the TTF species is dominant as the redox-active component and essentially nullifies the p-doping ability of the polythiophene backbone and precludes the possibility of polaron/bipolaron delocalization within the chain. From this viewpoint, one can question the rationale for designing such a structure—why limit the use of an organic semiconductor by switching off its

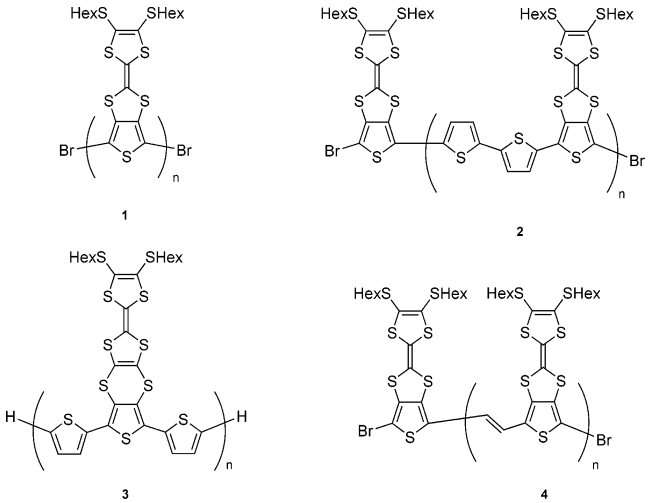

* To whom correspondence should be addressed. E-mail: peter.skabara@strath.ac.uk (P.J.S.). Present address: WestCHEM, Department of Pure and Applied Chemistry, University of Strathclyde, 295 Cathedral Street, Glasgow G1 1XL, Scotland (P.J.S.).

[†] University of Manchester.

[‡] Johannes Kepler University Linz.

[§] University of Newcastle.

10.1021/jp057256h CCC: $33.50
Published on Web 02/02/2006

SCHEME 1

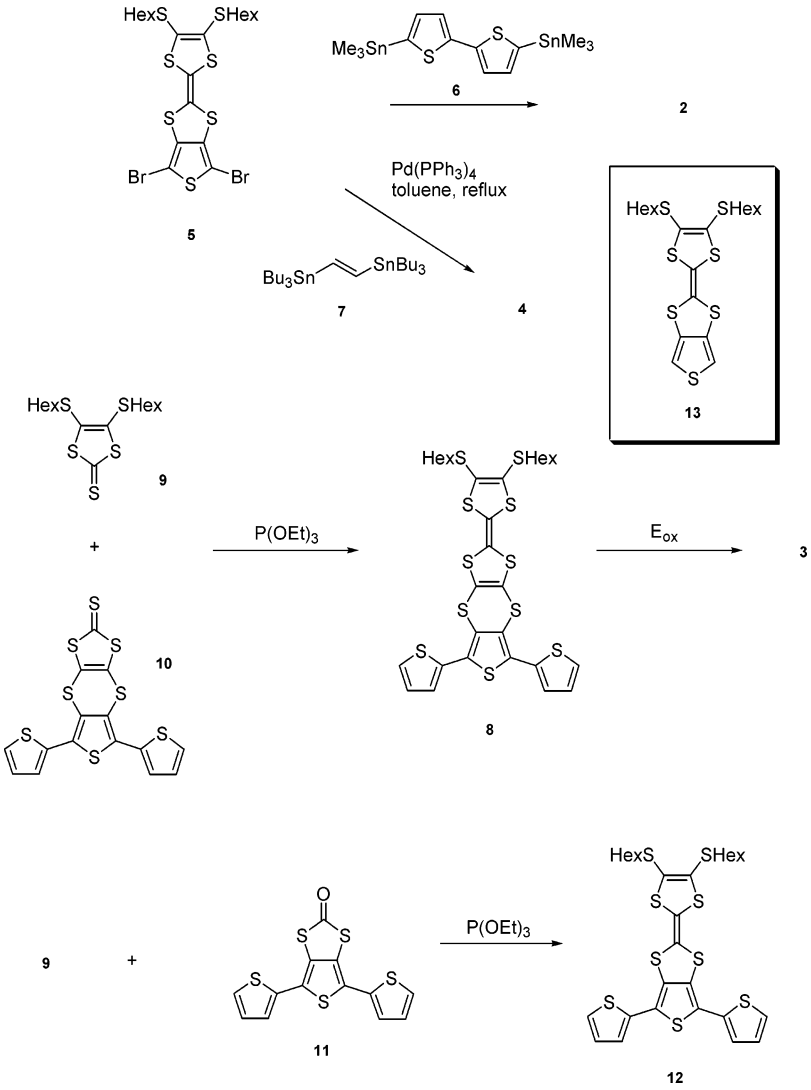

electroactivity or doping ability? A possible answer to this question is to provide a working example of such a material in a photovoltaic device and thereby present an intriguing example in which the dominant TTF unit can work in harmony with the "electroactively silenced" polythiophene moiety.

We report here a range of polythiophene−TTF derivatives (**2**−**4**) in which the TTF unit is sequentially, structurally withdrawn from the polythiophene chain. Spectroelectrochemical experiments on polymers **1**−**4** show that the TTF unit passes through various phases of electrochemical coparticipation with the polythiophene chain: dominant, hybrid, and then independent electroactivity. Photovoltaic devices have been fabricated and characterized from polymer **4**.

Results and Discussion

Synthesis. Polymers **2** and **4** were prepared from the reaction of dibromo derivative **5** with 5,5′-bis(trimethylstannyl)-2,2′-bithiophene (**6**)[35] and 1,2-bis(tributylstannyl)ethylene (**7**)[36] in toluene with $Pd(PPh_3)_4$ as the catalyst (55 and 41%, respectively, Scheme 1). The products were purified by Soxhlet extraction, using a series of solvents (methanol, acetone, and finally dichloromethane). Polymer **3** was obtained by electrochemical polymerization from the parent terthiophene **8**[37] (see the Electrochemistry section), which was in turn prepared from the reaction of compounds **9**[38] and **10**[39] in the presence of triethyl phosphite. In the same way, terthiophene **12** was prepared from the half-units **9** and **11**.[40]

The chemically prepared polymers **2** and **4** were characterized by gel permeation chromatography (GPC) against polystyrene standards in chloroform and the results indicated the presence of short chain polymers (**2**, $M_n = 4886$ and $M_w = 11740$; **4**, $M_n = 3158$ and $M_w = 3750$). Thiophene ring stretching vibrations are observed for all polymers (1412−1458 cm^{-1}) and are in the expected region for 3,4-annelated polythiophenes.[41,42] MALDI-TOF mass spectrometry was attempted on both polymers, but only **4** gave any meaningful results. The mass spectrum (see Supporting Information Figure S1) shows major peaks with mass differences corresponding to the repeat unit (TTF−thiophene and vinylene units, 516 mu). The spectrum clearly shows that **4** is end-capped with TTF−thiophenes and that the terminal bromine groups are intact. These results are also supported by the ^1H NMR ($CDCl_3$) spectrum of **4**, which confirms the absence of tributyltin groups in the polymer. The highest mass peak in the MALDI spectrum (5290) equates to 10 TTF−thiophene units in the polythienylenevinylene (PTV) chain, which is somewhat higher than the polymer weight deduced from the GPC results.

Thermogravimetric analysis was performed on polymers **2** and **4**, and as expected, the PTV system is less stable than the polyterthiophene analogue. Decomposition of **4** begins at 167

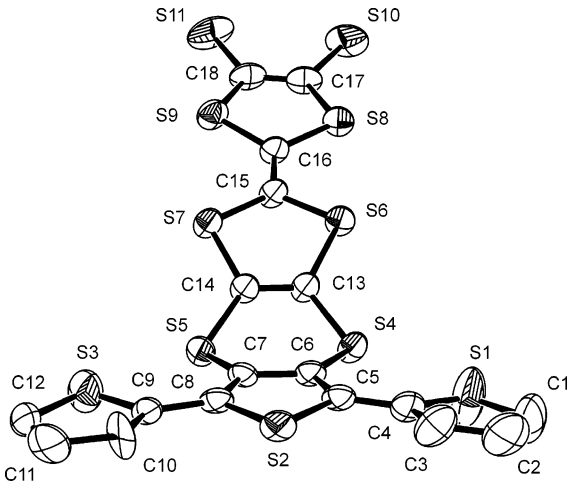

Figure 1. Molecular structure of compound **8** with hexyl chains and H atoms omitted. Displacement ellipsoids are drawn at the 50% probability level.

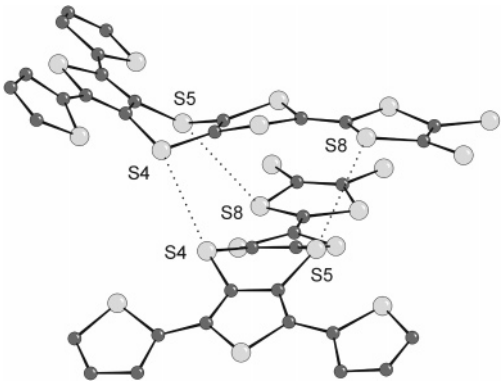

Figure 2. Dimers of **8** arising from close intermolecular S···S contacts.

°C, with an 8% weight loss by 251 °C. Further, accelerated decomposition occurs after this point and an overall weight loss of 40% is achieved by 312 °C. For polymer **2**, 40% weight loss occurs within the range 227−400 °C.

X-ray Crystallography. Terthiophene **8** provides a good example for chalcogen intramolecular interactions that promote planarity in the main chain of oligomeric conjugated architectures.[43−46] This structural feature is expected to predominate in corresponding polymer films and is therefore conducive to the attainment of high conjugation and a low band gap state. Compound **8** was recrystallized from dichloromethane−hexane to give an orange crystalline solid; however, the small size of the crystals (∼0.02 mm) and disorder in one of the hexyl groups led to very weak diffraction, requiring the use of synchrotron radiation for a successful structure determination. The molecular structure of the terthiophene is shown in Figure 1.

The hexyl chain appended to atom S10 is disordered and appears to be highly distorted, whereas that attached to S11 assumes the typical zigzag motif of an alkyl chain. The terthiophene moiety adopts an all-trans conformation with a reasonably high degree of coplanarity between the thiophene units. The maximum torsion angles between rings are 167.3(4)° (S1−C4−C5−S2) and −173.4(6)° (C7−C8−C9−C10). As seen in previous examples of terthiophenes bearing dithio derivatives,[40] there are significant intramolecular S···S interactions between the sulfurs of the peripheral thiophenes and the sulfur substituents at the 3,4-positions of the central ring. The contacts are significantly shorter than the sum of the van der Waals radii for two sulfur atoms (3.60 Å)[47] at S3···S5 = 3.182(2) Å and S1···S4 = 3.187(3) Å, and such interactions are regarded as strongly influential in the planarization of conjugated systems.[48] As expected for the majority of neutral dithiin structures,[49,50] the dithiin ring adopts a boat conformation with a folding of 48.8(2)° along the S4···S5 vector. The two dithiole units are approximately coplanar, with *cis*-S−C15−C16−S torsion angles of 4.0(7) and 3.9(8)°. The molecules form dimers in the crystalline state through S4···S4′ (3.42 Å) and S5···S8′ (3.65 Å) intermolecular contacts. There are no further significant intermolecular contacts observed in the packing of **8**.

TABLE 1: Electrochemical Data for Monomers and Polymers[a]

	$E_{1ox}^{1/2}$ V vs Fc/Fc$^+$	$E_{2ox}^{1/2}$ V vs Fc/Fc$^+$	$E_{red}^{1/2}$
12	+0.64	+1.02	
8	+0.64	+0.99	
5	+0.95	+1.31	
13	+0.74	+1.10	
1	+0.81	+1.10	−1.15[irr]
2 (solution)	+0.69	+1.07	−1.65[q]
3 (solid state)	+0.77	+1.09	−1.21[irr]
4 (solution)	+0.89	+1.31	
4 (solid state)	+0.91[irr]	+1.35[irr]	−0.73[q] (0.49 V difference)

[a] CH_2Cl_2, 0.1 M Bu_4NPF_6, 100 mV s^{-1}; [irr]irreversible peak; [q]quasi-reversible peak.

Electrochemistry. The electrochemical behavior of compounds **8**, **12**, and **13** is presented in Table 1. All three compounds show two sequential, reversible oxidation waves corresponding to the formation of the TTF radical cation and dication, respectively. It is noteworthy that the oxidation values for the two terthiophene derivatives are almost identical, thereby demonstrating that any inductive effect due to the 1,4-dithiin ring is negligible. However, each oxidation of the TTF moiety in **13** is shifted to a more positive value by ∼100 mV, compared to derivatives **8** and **12**. The electronic effect of the fused thiophene ring upon the TTF unit can be explained by a σ-electron-withdrawing effect in **13**, which is reduced by a counteractive π-resonance effect of the two peripheral thiophene rings in **8** and **12**.

For electropolymerization experiments, repetitive scanning over the range 0.0 to +1.6 V was performed, using a Ag/AgCl reference electrode and a gold disk working electrode in a dichloromethane−hexane (2:1) solution containing tetrabutylammonium hexafluorophosphate (0.1 M) as the supporting electrolyte. As we have observed previously,[51] monomer **13** failed to polymerize; however, we were quite surprised to discover different electrochemical reactivities for compounds **8** and **12**, despite the close similarity in redox potentials. Although, in the case of **12**, we observed the formation of a red film on the surface of the electrode, cyclic voltammetry clearly showed that this was not of polymeric nature. Conversely, reproducible films of polymer **3** were obtained from monomer **8** under identical conditions[37] (a typical trace showing polymer growth over 10 cycles can be seen in Supporting Information Figure S3). The proportionally higher increase in current between scans for $E_2^{1/2}$ compared to the first oxidation wave has been seen previously in poly(bithiophenes) linked to TTF units via saturated spacer groups.[52] This type of behavior shows that the second oxidation of the TTF species develops independently of charge transport through the film, which is not the case for $E_1^{1/2}$.

The electrochemical behavior of the polymers (**2**−**4**) has been studied by cyclic voltammetry in solution and as thin films deposited on gold or indium tin oxide (ITO) working electrodes. The results are summarized in Table 1. All compounds and

TABLE 2: Electronic Absorption Data for Polymers 1−4 and Related Monomers

	solution (CH_2Cl_2) λ_{max} (nm)	thin film λ_{max} (nm)	electronic band gap in solid state (eV)	electrochemical band gap (eV)
12	373			
8	344			
5	337			
13	324			
1[34]	466	487	1.75	1.82
2	456	496	1.82	1.83
3	486	494	1.7	1.81
4	578	598	1.45	1.44

polymers give two sequential, reversible oxidation waves in the region +0.64 to +1.35 V. There is a marked difference in the oxidation potentials for the polymers: in each case, E_{1ox} and E_{2ox} are higher than the corresponding values for the simple monomer systems (**8**, **12**, and **13**), with the largest change following the sequence **4** > **3** > **2**. In fact, the redox potentials for polymer **4** are very close to those for dibromo monomer **5**. There is a greater variance in the reduction potentials for polymers **2**−**4** (Table 1), and these processes are either irreversible or quasi-reversible.

The most pertinent question concerning the electroactivity of the polymers is the assignment of electron donating sites within these structures, since the conjugated main chain could easily be responsible for the redox behavior of the polymer. To this end, we have conducted spectroelectrochemical measurements (ultraviolet−visible (UV−vis) and electron paramagnetic resonance (EPR)) on polymers **2**−**4** and performed computational studies to identify the precise oxidation sites within the macromolecules (see later sections). However, the exceptional and unprecedented doping level observed for polythiophene **1**[34] is also displayed by polymers **2**−**4**. From bulk electrolysis experiments utilizing a platinum gauze working electrode, the number of electrons removed per repeat unit from **2**−**4** was found to be approximately two. Naturally, the highest charge density is achieved with polymer **4**.

Determination of Band Gaps. Absorption spectra were obtained in solution and, for the polymers, in solid state form on ITO glass. The data are collated in Table 2. Polymers **1**−**3** have very similar absorption characteristics, displaying maxima in the range 456−466 nm in dichloromethane and 487−496 nm in the solid state. The electronic band gaps are also close (1.7−1.8 eV) and are less than the band gap for unsubstituted polythiophene (2.0 eV) and similar to poly(3-hexylthiophene) (1.7 eV).[53] The spectra indicate that the dithiin ring in **3** does not affect the electronic properties of the polymer, since the absorption characteristics are similar between **2** and **3**. Furthermore, the absorption maxima for **2** and **3** are very close to those for polymer **14** (478−489 nm, solid state),[40] indicating that the TTF and dithiin heterocycles possess similar substituent effects. From this observation, one would expect that the absorption characteristics of **1** should also be comparable to PEDTT. However, the latter has an absorption maximum at 396 nm and a considerably higher band gap of 2.42 eV. Clearly, the TTF-based polymer does not mirror the properties of PEDTT, which

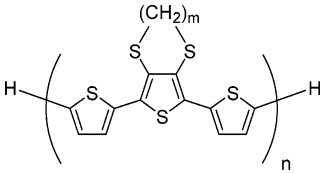

14 m = 1, 2, 3

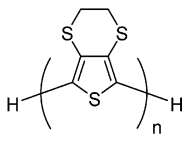

PEDTT

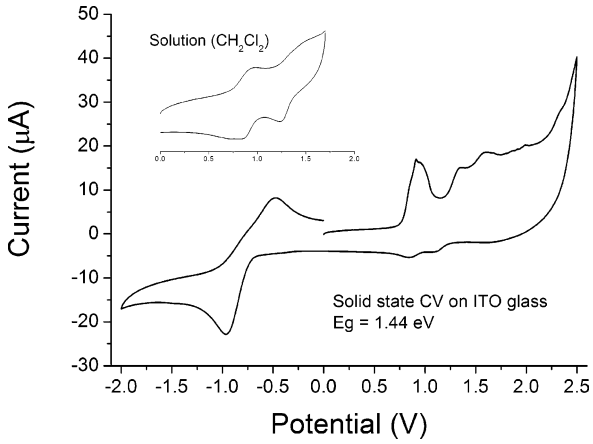

Figure 3. Cyclic voltammograms of polymer **4** in solution and as a thin film.

suffers from a deviation from coplanarity between repeat units,[54] due to steric repulsion between the sulfur atoms of the six-membered ring in comparison to the five-membered unit in **1**.

As expected for a polythienylenevinylene system, the absorption maximum of polymer **4** is red-shifted in comparison to polymers **1**−**3**. In the solid state, the longest wavelength absorption band has an onset at 854 nm, which equates to an optical band gap of 1.45 eV. Treatment of a solution of polymer **4** with hydrazine does not affect the absorption characteristics of the polymer, indicating that the isolated material is undoped and stable under ambient conditions.

For simple polythiophene structures, band gaps can be deduced by cyclic voltammetry from the difference of the onset of oxidation and reduction processes. For our TTF−polythiophenes, the situation is more complicated and we have seen that in polymer **1** the relationship between electrochemical and electronic band gaps does not reach parity unless one assumes that the first oxidation process is independent of the polymer chain and, therefore, the onset of the second oxidation process is considered.[34] This assumption is quite reasonable, since one would expect the first oxidation to take place within the more electron-rich 1,3-dithiole (bearing alkylsulfanyl substituents) and that the second TTF half-unit is associated more intimately with the polymer chain. For polymers **2**−**4**, we have observed the same situation; the difference between the second oxidation wave and the reduction wave for each polymer gives us values that agree very closely with the band gaps derived from absorption studies (see Table 2). In the solid state, the cyclic voltammograms display quite different redox behavior, which is attributed to charge trapping and interchain interactions. Solution state and solid state voltammograms for polymer **4** are shown in Figure 3. The reversibility of the oxidation processes is greatly diminished in the solid state, and in this case, the difference between the onset of the first oxidation wave and that of the reduction wave gives the true electrochemical band gap. This change in electronic behavior could be due to significant interactions taking place in the solid state, and we tentatively suggest that this could be due to intermolecular charge transfer between the polymer chains and the oxidized TTF unit.

Spectroelectrochemistry. UV−vis spectroelectrochemical (SEC) measurements were performed on thin films which were spin-coated (**2** and **4**) or electrodeposited (**3**) onto ITO glass. All experiments were conducted in acetonitrile solution at a potential range which covered the neutral states of the polymers and both oxidation processes observed in the cyclic voltammo-

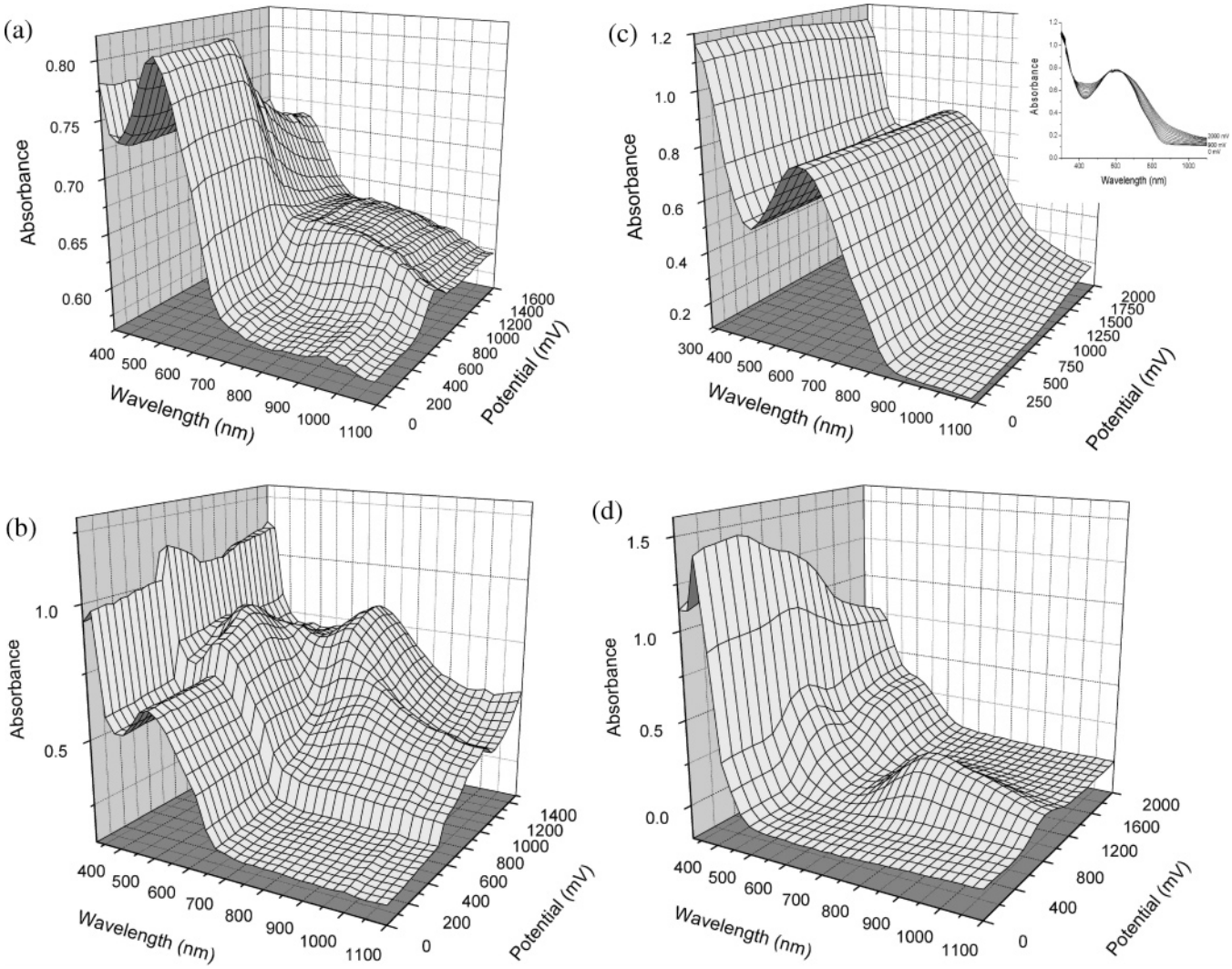

Figure 4. UV−vis spectrolectrochemical measurements performed on polymers **2** (a), **3** (b), and **4** (c) and compound **12** (d).

grams of the materials. The results are depicted in Figure 4a−c. Previous spectroelectrochemical studies conducted on TTF and its derivatives[34,55−57] have identified several unique absorption characteristics derived from the oxidized TTF units. The product from the first oxidation process, $TTF^{\bullet+}$, usually gives rise to two new absorption bands (430 and 580 nm for TTF itself). These new peaks are often accompanied by a third band at ~800 nm, which can be assigned to an intermolecular charge transfer process between $TTF^{\bullet+}$ dimers or as an additional feature of the cation radical species.[58] Once the molecule is oxidized to the dication, these peaks disappear and a new band emerges at lower wavelengths (390 nm for TTF^{2+}).[55] In all of the spectra, the absorption peaks of polymers **2**−**4** extend to approximately 680−850 nm, which precludes the identification of the TTF dication and the two lowest wavelength absorption bands of the cation radical. Oligomer **15**[59] provides a good model for the spectroelectrochemical behavior we would expect to see from polymers **2** and **3** if the TTF unit was electrochemically inert. For compound **15**, new bands emerge at 651 and >1100 nm when the potential surpasses that of the cation radical and dication states and the static behavior of the absorption band, which corresponds to the $\pi-\pi^*$ transition of the conjugated chain, suggests strong participation of the alkylsulfanyl groups in delocalizing the charged intermediate state.[59] Between polymers **2** and **3** (Figure 4a and b), we observe dissimilar absorption behavior, and there is little comparison to be made with the spectrum of **15**. As the potential is raised, polymer **2** gives rise to a very broad and ill-defined band extending from 700 to 1100 nm. Oxidation of the TTF units is expected and charge transfer processes between adjacent $TTF^{\bullet+}$ species could be responsible for this broad band. However, since the bulk electrolysis experiments show that each TTF unit in the polymer chain is oxidized, this charge transfer process should not be possible. Alternatively, the charge transfer process could reside between the TTF fragments and the polythiophene chains; in such a situation, we would have considerable charge delocalization throughout the whole macromolecule, which would explain the broad nature of the new band. Since compound **12** is inert to oxidative electropolymerization, we were able to conduct a spectroelectrochemical assay of the isolated repeat unit of **2** (Figure 4d; experiment conducted in dichloromethane solution). The first oxidation process gives rise to a band at 797 nm, indicating the presence of the $TTF^{\bullet+}$ species. This feature disappears sharply with the onset of the second oxidation event, along with the concomitant growth of a peak centered at 509 nm (dication). In contrast to the SEC trace of polymer **2**, these bands are clearly defined and provide further evidence of charge delocalization in the main chain of **2**. Although the main $\pi-\pi^*$ bands for **2** and **12** diminish during oxidation, they remain the most intense peaks in both spectra.

In the spectrum for polymer **3**, the emerging absorption bands are more finely resolved than those of **2** and we initially see a new peak arising at 814 nm. Although this could be due to charge transfer between cation radical dimers (as seen for

$TTF^{\bullet+}$), a similar peak is observed in the spectroelectrochemistry of polymer **16** (859 nm),[60] in which the quinoxaline unit is inert under oxidative conditions. As the potential is increased, the band at 814 nm for **3** is lost and a second band grows at 653 nm, along with the gradual loss of the peak at 494 nm. This behavior is very similar to that of polymer **16**, which at higher potentials has a new band emerging at 660 nm, accompanied by a hypsochromic shift of the $\pi-\pi^*$ band from 475 to 380 nm. For polymer **16**, we assign this sequence of events to the sequential formation of polarons and bipolarons within the polymer chains and on the basis of this evidence we believe that the oxidation processes in polymer **3** take place within both electroactive units, namely, the polythiophene chain and the TTF side group. In the case of polymer **4**, the spectroelectrochemistry is remarkably featureless, with only a small increase in absorbance within the shoulders of the main absorption peak centered at 598 nm. Again, we expect the oxidation processes to derive from the TTF units, with some possible delocalization over the conjugated chain. However, it is quite astonishing that the $\pi-\pi^*$ band remains completely unchanged throughout the experiment, even up to +2.0 V, indicating that the conjugated chain is perfectly preserved and electrochemically inert. This raises a very interesting question, since, if the electroactivity of the polymer chain is switched off, then how will the material behave as a semiconductor? This quandary is answered in a later section, in which polymer **4** is used as an active component with [6,6]-phenyl-C_{61} butyric acid methyl ester (PCBM) in a solar cell device.

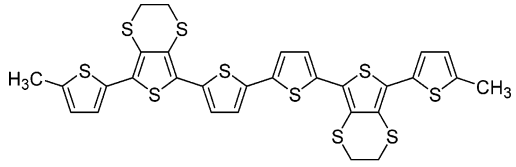

15

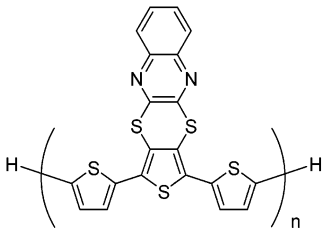

16

The electrochemical polymerization of **3** was investigated by EPR spectroelectrochemistry. EPR spectra were recorded at X-band (9.4 GHz) on a Bruker EMX spectrometer. Compound **8** was dissolved in CH_2Cl_2 containing tetrabutylammonium hexafluorophosphate (0.1M) as the supporting electrolyte. The solution was transferred to a flat cell provided with a platinum gauze working electrode, a platinum wire counter electrode, and an Ag/AgCl reference electrode. The spectrum was recorded every 10 min at a fixed voltage. At a potential of +0.64 V (room temperature, Figure 5a), a single line is observed at $g_{iso} = 2.0077$ with weak satellites. The spectrum can be simulated (Figure 5a) assuming coupling to a single ^{33}S nucleus but at 4 times the natural abundance of ^{33}S, because there is a probability of 4×0.76 of having a single ^{33}S nucleus in the $TTF^{\bullet+}$ moiety. On freezing the solution to 120 K, a rhombic set of g values is observed, $g_1 = 2.003$, $g_2 = 2.007$, and $g_3 = 2.011$. Both the isotropic (g_{iso}, A_{iso}) and anisotropic parameters are very similar

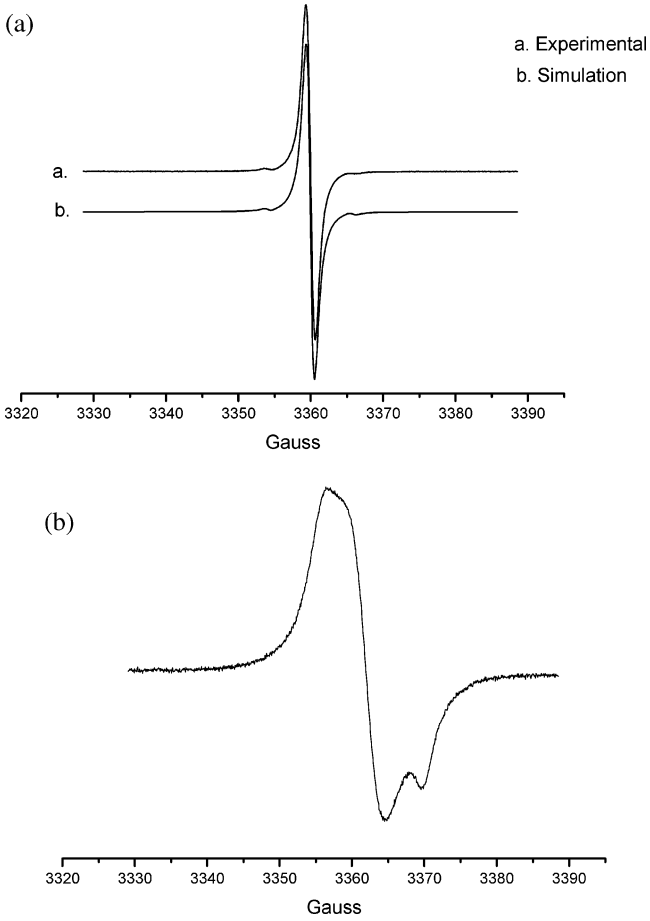

Figure 5. (a) EPR spectrum of **8** at +0.64 V and at room temperature ($g_{iso} = 2.0077$, $A_{iso}(^{33}S) = 3.9$ G). (b) EPR spectrum of **8** at +0.64 V and at 120 K ($g_1 = 2.003$, $g_2 = 2.007$, $g_3 = 2.011$).

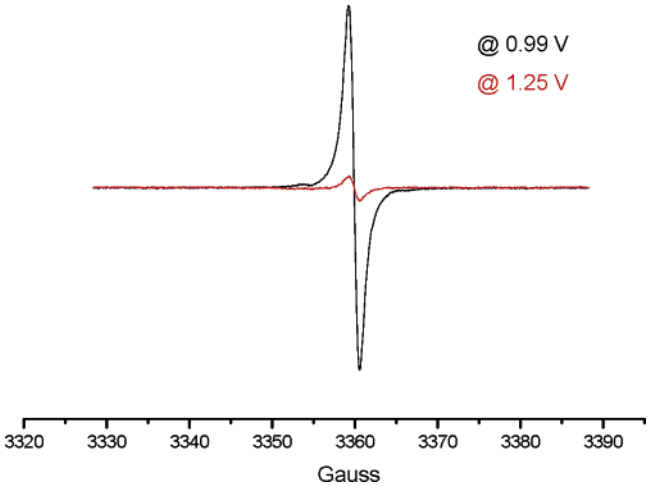

Figure 6. EPR spectrum of polymer **3** at +0.99 and +1.25 V.

to those of $TTF^{\bullet+}$ itself,[61] confirming that the TTF moiety in **8** is the redox-active unit.

As the potential is increased, the observed signal diminishes rapidly (Figure 6 of the spectrum at +1.25V) and no new signal grows in fluid and frozen solution. This is consistent with the oxidation of $\mathbf{8}^{\bullet+}$ to $\mathbf{8}^{2+}$, although it gives no direct evidence on the nature of the second oxidation process (see later). The EPR spectra of **2** and **4** were also recorded at potentials over $E_1^{1/2}$ for each of the polymers, and in both cases, the g values were found to be 2.005.

	Charge	Multiplicity
d	2	1
c	2	3
b	1	2
a	0	1

Figure 7. Optimized geometry for **8** in its various charged states.

	Charge	Multiplicity
d	2	1
c	2	3
b	1	2
a	0	1

Figure 8. Optimized geometry for **12** in its various charged states.

Computational Studies. All calculations were carried out using the Gaussian 03 suite of programs.[62] The geometries of the monomer units were optimized using the B3LYP hybrid functional with a 6-31G(d) basis on carbon, hydrogen, and sulfur. To answer the question of whether the TTF unit acts independently from the main electroactive chain, calculations were performed on the ground state and oxidized states of monomers **8** and **12**. The hexyl chains were omitted for reasons of computational cost. It was found that omitting the hexyl chains had a negligible effect on the geometry of **8** (see Supporting Information Figure S4). In our studies, the geometry was optimized for the neutral singlet state, the cationic doublet state, and the dicationic triplet and singlet states. This corresponds to the redox behavior of the TTF unit which is a two-electron donor.

The torsion angles and relative energies of the singlet and triplet states of the dication are given in the Supporting Information (Supporting Information Figure S5 and Tables T1 and T2). Most noteworthy is the planarization of **12c** (Figure 8) which should maximize the possibility of $\pi-\pi$ stacking in the bulk material. From our calculations on the dication species, we note that the singlet state is less stable than the triplet configuration. The relaxation energy, defined as the difference in energy between the ion state at its optimized geometry and the ground state geometry, is given in Table 3.

TABLE 3: Relaxation Energy for Compounds 8 and 12[a]

	relaxation energy/kJ mol^{-1}		
compound	GS → cation	cation → dication (triplet)	cation → dication (singlet)
8	22.4	35.9	22.5
12	24.5	23.5	18.6

[a] GS denotes the neutral species.

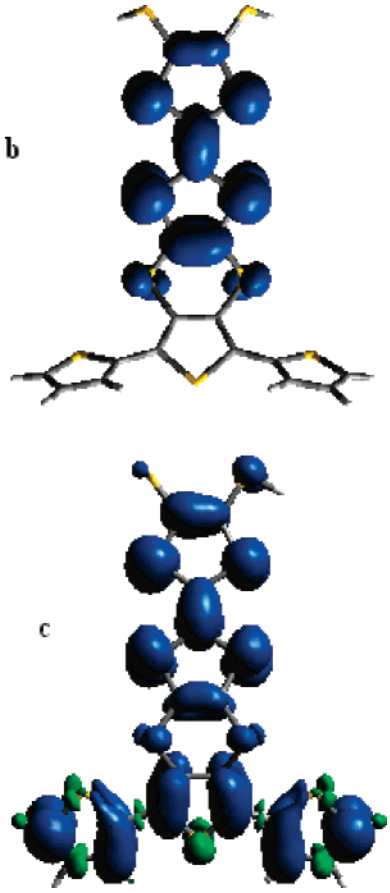

Figure 9. Spin density of the **8b** cation doublet and the **8c** dication triplet.

Returning to the question of whether TTF imparts electronic character into the terthiophene unit, CIS and time-dependent density functional theory (DFT) calculations were performed. From the calculated absorption spectra, the principal electronic transitions were often observed to be between the TTF and thiophene moieties. This strongly indicates conjugation. The spin densities for the compounds were investigated (Figures 9 and 10), and it was found that, for the monocationic state, the spin is only delocalized on the TTF unit. Modeling the dicationic state, the triplet state was found to be more stable and the spins were found to be delocalized over the whole molecule, indicating that the different electroactive units interact with each other. The spin density is essentially composed of the two singly occupied molecular orbitals (SOMOs) which are located on different units.

The question arises of whether conjugation requires that the two electrons occupy different orbitals and to what extent conjugation is affected in the singlet state in which two electrons can share the same spatial orbital. Accordingly, we carried out spin-unrestricted calculations at the UB3LYP/6-31G(d) level. The S^2 operator can be used to assess whether in the singlet state an open-shell singlet structure is obtained (with the highest

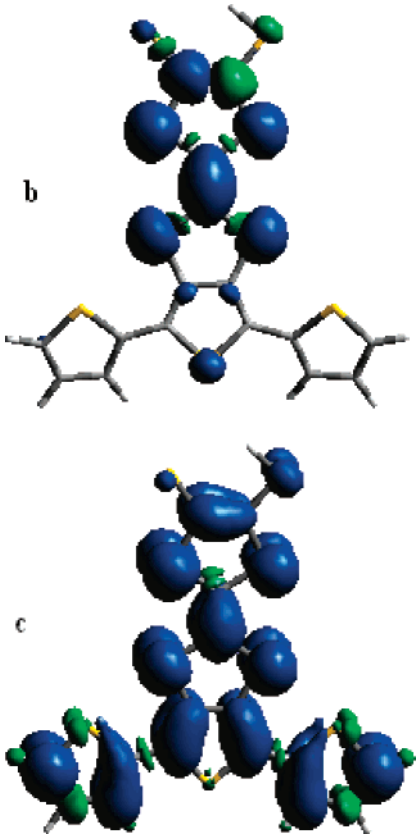

Figure 10. Spin density of the **12b** cation doublet and the **12c** dication triplet.

TABLE 4: $\langle S^2 \rangle$ Values and Relative Energies of Dication States of 12 and 8

compound	multiplicity	S^2	energy/kJ mol^{-1}
12	triplet	2.0255	0.00
12	singlet	0.9967	11.01
8	triplet	2.0223	0.00
8	singlet	1.0217	0.21

TABLE 5: Eigenvalues for SOMOs of Compounds 8 and 12

compound	reference	eigenvalue/eV
8	Figure 11a	−10.91
8	Figure 11b	−11.17
12	Figure 12a	−11.51
12	Figure 12b	−11.61

lying α and β spin orbitals being spatially distinct). The wave functions of pure spin states obey eq 1:

$$S^2|\omega\rangle = S(S+1)|\omega\rangle, \text{ where } S = {}^1/_2(n_\alpha - n_\beta) \qquad (1)$$

For pure spin states, we would expect values of $\langle S^2 \rangle$ of 0 for singlets and 2 for triplets. An open-shell singlet will have a value of $\langle S^2 \rangle \approx 1$, indicating a mixing of singlet and triplet states.

Compounds **8** and **12** show the triplet state to be lowest in energy for the dication. However, conjugation can arise in both the triplet and singlet states. Table 5 shows that the $\langle S^2 \rangle$ eigenvalues for the singlet states are close to 1, indicating an open-shell singlet. Inspection of the highest occupied molecular orbitals (HOMOs) of α and β spin (see Figure 13 for **8**) clearly shows that the orbitals are spatially distinct and localized on the different electroactive units. Hence, conjugation between TTF and thiophene can occur in either singlet or triplet states for **8** and **12**. Indeed, in **8**, the energy difference between singlet and triplet states is calculated to be only 0.2 kJ mol^{-1}.

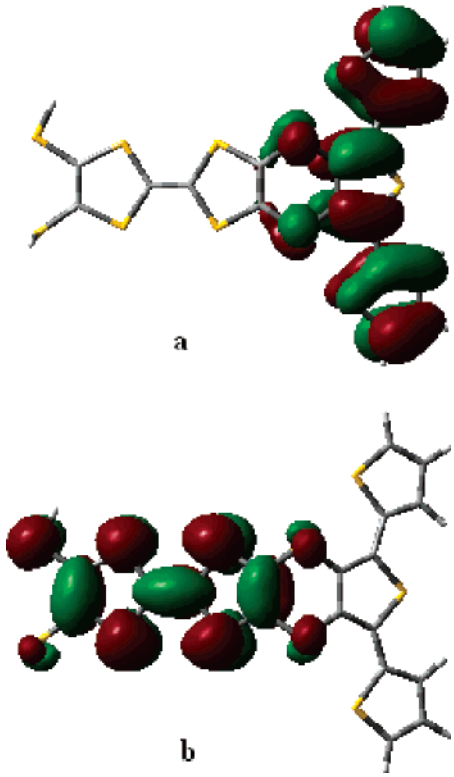

Figure 11. The two singly occupied molecular orbitals for **8** in its triplet dicationic state. This is with reference to the spin density in Figure 9c. Note that a < b in energy.

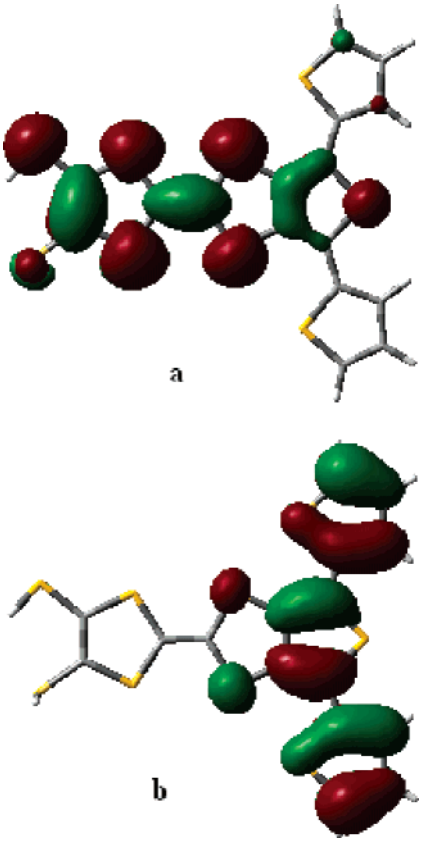

Figure 12. The two singly occupied molecular orbitals for **12** in its triplet dicationic state. This is with reference to the spin density in Figure 10c. Note that a < b in energy.

From the previous section, EPR studies of $\mathbf{8}^{+\bullet}$ indicated that the spin resides on the TTF part of the molecule, and this is supported by the calculations. As the potential is raised beyond the second oxidation peak to form $\mathbf{8}^{2+}$, the signal disappears. Although, $\mathbf{8}^{2+}$ is EPR silent at room temperature and 120 K, this cannot give direct evidence on the nature of the ground state; if the triplet state is populated either as the ground state or as a thermally accessible excited state, then the absence of the spectrum would indicate rapid relaxation of the triplet at the experimental temperatures. However, obviously an EPR silent species would also be consistent with both redox processes, successively depopulating the same orbital. Therefore, the EPR is inconclusive on the nature of $\mathbf{8}^{2+}$. Beyond the cation state, there is still reasonable doubt as to the configuration in which the compounds exist experimentally. However, the UV−vis spectroelectrochemical experiments clearly show that electrons are removed from both electroactive units in polymers **2** and **3**.

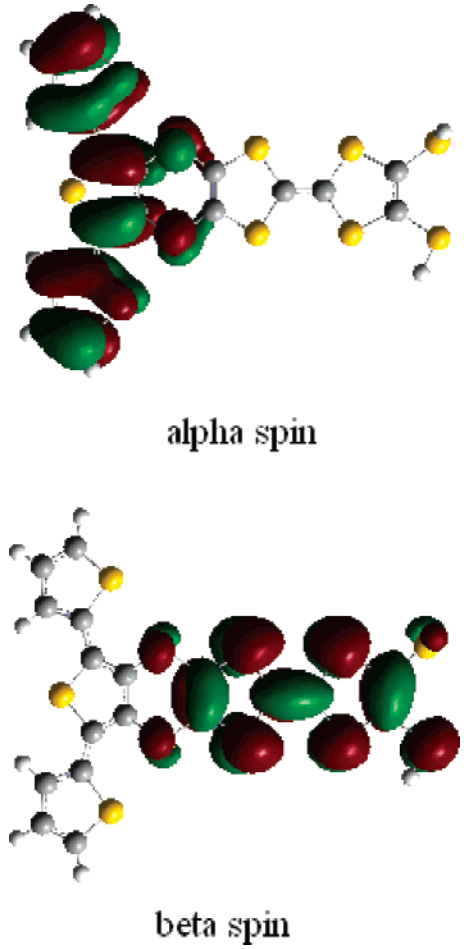

Figure 13. The HOMO spin orbitals in the spin-unrestricted singlet calculation on **8**.

Photoluminescence and Photoinduced Absorption Spectra of Polymer 4. Thienylenevinylene-based oligomers[63−66] and polymers[67,68] have been studied in the past few years as promising candidates for low band gap materials. Optical absorption onsets <1.5 eV have been reported for such material systems.[69] The absorption characteristics of **4** are compared with the emission spectrum in Figure 14 (excitation wavelength 514 nm). The main longest wavelength absorption peak shows a maximum around 630 nm and an onset around 850 nm. The photoluminescence is weak and shows a broad maximum at 800 nm and a relatively sharp peak at 670 nm. The origin of the 670 nm peak in the photoluminescence spectrum is unclear, and the absorption and photoluminescence spectra are overlapping. A similar effect has been reported for poly(2,5-

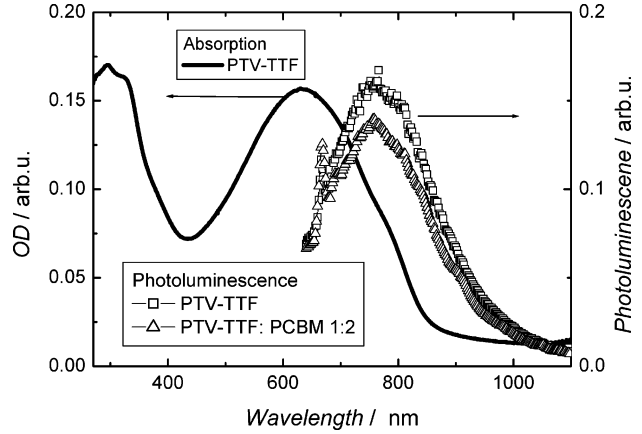

Figure 14. Absorption and photoluminescence of a thin film of polymer **4**. In comparison, the photoluminescence of a 1:2 PTV-TTF **4**:PCBM blended film is shown. Photoluminescence spectra were recorded at 80 K, excitation with 40 mW, and 514 nm.

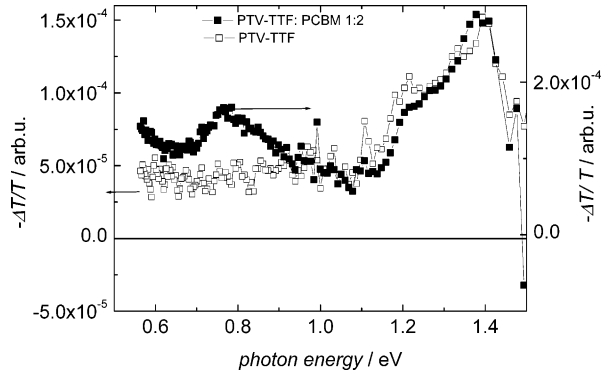

Figure 15. PIA spectrum of PTV−TTF **4** and 1:2 PTV−TTF: **4**:PCBM thin films, drop-cast on glass. Spectra were recorded at 20 K, illumination at 514 mW with 40 mW.

thienylenevinylene) films.[70] The photoluminescence of **4** is preserved in blends with [6,6]-phenyl-C_{61} butyric acid methyl ester (PCBM).

From the electrochemical measurements, the energy values for the HOMO and lowest unoccupied molecular orbital (LUMO) of polymer **4** are −5.24 and −3.78 eV, respectively. The LUMO of **4** shows only a small energy offset to the LUMO of PCBM (−3.75 eV),[71] and from this point of view, the energetic possibility for photoinduced electron transfer from **4** to PCBM is unclear. The photoinduced absorption (PIA) spectrum of **4** (see Figure 15) shows a peak at 1.35 eV with a shoulder at 1.2 eV. In the near-infrared region between 1.0 and 0.6 eV, a significant offset without any distinct feature is observed. The modulation frequency dependences of the PIA at 1.38 and 1.22 eV are weak, and no crossing of the in-phase and out-of-phase signals is observed (Figure 16). This indicates relatively short lifetimes (τ < 0.1 ms) with a broad inhomogeneous distribution. No model could be found to fit this modulation dependence satisfactorily. The PIA spectrum of a **4**:PCBM blend film is shown in Figure 15. The 1.4 eV PIA of the pristine polymer is preserved in the blend, but additionally, two new absorption peaks at 0.8 and <0.55 eV are observed.

The modulation frequency dependences (Figure 17) show slight differences for the 1.4 eV band and new absorptions at 0.8 and <0.55 eV. The peak at 1.46 eV could be fitted by the dispersive recombination model with a mean lifetime of τ = 0.7 ms. The lifetime shows a broad distribution (α = 0.64). The two low energy peaks show a weaker dependence on the modulation frequency, indicating shorter lifetimes. Excited state

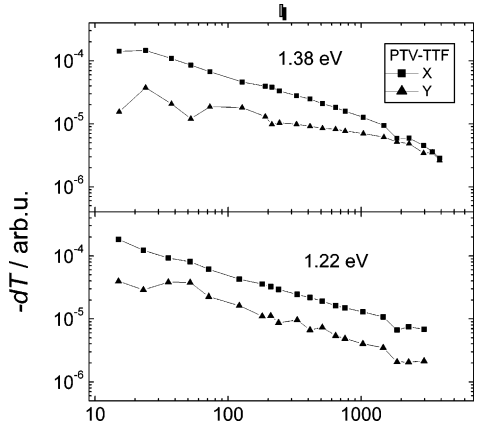

Figure 16. Modulation frequency dependence of the PIA of PTV-TTF **4** at 1.38 eV (upper part) and 1.22 eV (lower part). The measurements were done at 20 K with illumination at 40 mW.

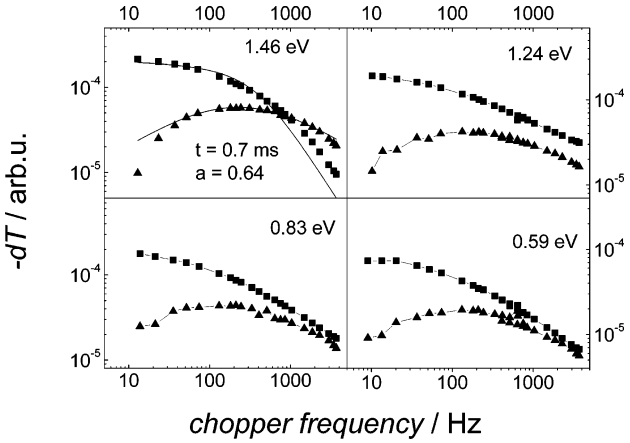

Figure 17. Modulation frequency dependence of the PIA of 1:2 PTV-TTF **4**:PCBM at 1.46, 1.24, 0.83, and 0.59 eV. The measurements were carried out at 20 K with illumination at 40 mW. For 1.46 eV, an excited state lifetime of 0.7 ms and a dispersion factor of α = 0.64 were calculated. For the other measurements, the fitting procedure does not lead to a satisfying result.

interactions between oligothienylenevinylenes and fulleropyrrolidines (MP-C_{60}) in solution have been investigated by Apperloo et al.[72] The PIA spectra for **4** and the blend with PCBM are compared with spectra for hexyl-substituted dodeca(thienylenevinylene) (12TV): MP-C_{60} mixed solution. The optical absorption of 12TV in CH_2Cl_2 shows a maximum at 2.11 eV, compared with 2.06 eV for **4** in chlorobenzene solution. In the solid state, the absorption maximum is shifted to 1.96 eV. PIA of 12 TV and MP-C_{60} in the nonpolar solvent toluene shows a peak at 1.42 eV. This peak is assigned to a $T_1 \rightarrow T_n$ absorption of triplet excited 12TV. In the more polar solvent *o*-dichlorobenzene, two additional peaks at 0.46 and 1.00 eV are observed in addition to the 1.42 eV peak. These two new absorptions are assigned to the 12TV radical cation. This assignment is confirmed by in situ electrochemical absorption measurements.[73] Furthermore, for polythienylenevinylene polaron absorptions were determined by Lane et al. by photoinduced absorption detected magnetic resonance at 1.1 and 0.4 eV.[74] Apperloo et al. determined that the triplet and charge-separated states of 12TV possess comparable energies. It is therefore assumed that the triplet state of 12TV and the charge-separated state can be formed and observed simultaneously.[73] In the PIA for both materials, a peak at 1.4 eV is observed. This peak was assigned to a $T_1 \rightarrow T_n$ absorption. Furthermore, the 0.8 eV and <0.55 eV peaks are comparable with the cation

SCHEME 2

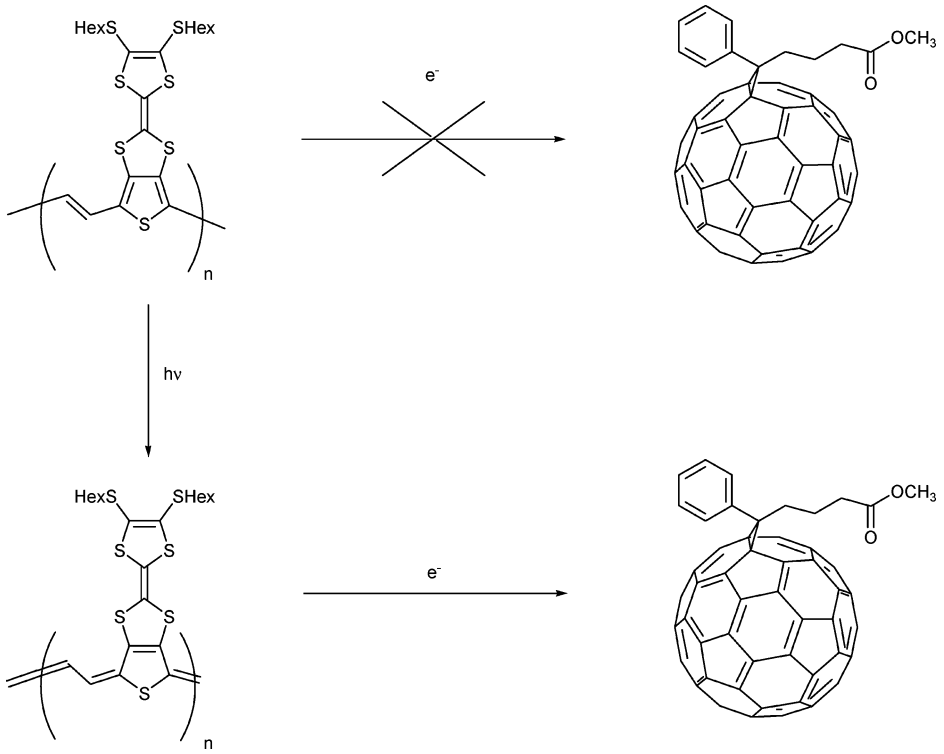

absorption of 12TV at 1 and 0.46 eV and therefore assigned to the polaron absorption of **4**. Similar to the optical absorption, a red shift is observed for the positive polaron. In blends of **4** and PCBM, the coexistence of triplet and charge-separated states is deduced.

Photovoltaic Device Work from Polymer 4. Pristine **4** shows nonuniform film forming properties, and therefore, no reliable electro-optical characterization could be obtained. In combination with PCBM, thin films of sufficient quality can be spin-cast from chlorobenzene solution. The I−V characteristics show diode rectification behavior with a rectification factor of $R(\pm 2\ \mathrm{V}) = 250$ (Figure 18). Under illumination, a photovoltaic effect is observed with a power conversion efficiency of 0.13% under AM1.5 solar simulated light. This is comparable with literature values reported for polythienylenevinylene-based bulk heterojunction devices.[75] The photocurrent spectrum (Figure 19) shows peaks at 350 and 650 nm, corresponding to PCBM and **4** absorption, respectively. The onset for the photocurrent is around 850 nm, corresponding to the absorption onset of **4**. As such, the optical response of the solar photovoltaic devices is improved to lower band gaps; however, the nanomorphology has to be engineered and the charge carrier mobility has to be improved to obtain higher current densities.

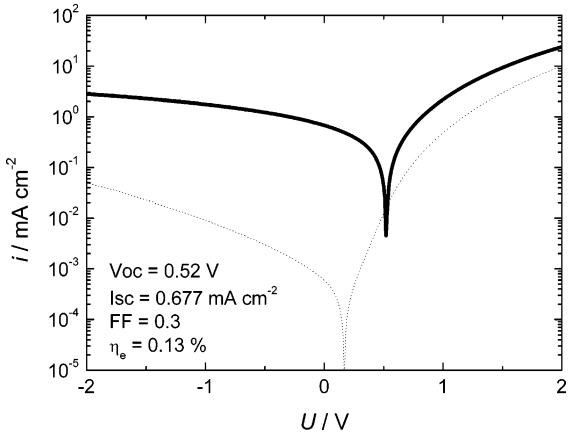

Figure 18. Current−voltage characteristics for a 1:2 PTV-TTF **4**:PCBM device, spin-coated from chlorobenzene, in the dark (dotted line) and under illumination from a solar simulator with 80 mW cm^{-2}. The active area thickness is approximately 50 nm.

Conclusions

In this paper, we have presented a new family of polythiophenes with repeat units bearing a TTF unit fused to the backbone of the thiophene chain. Polymers **1** and **4**, bearing the highest concentration of TTFs fused directly to the conjugated chain, are unique in that the absorption characteristics are derived from the polythiophene but the electroactivity is dominated by the tetrathiafulvalenes. By altering the structure of the repeat unit between polymers **1** and **2**, we have diluted the concentration of the TTFs and observed a broadening in the longest wavelength absorption band upon p-doping. This

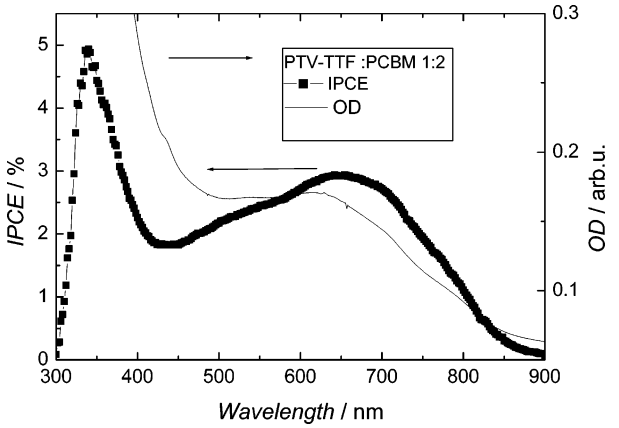

Figure 19. Photocurrent spectrum of a 1:2 PTV−TTF **4**:PCBM device, in comparison with the optical absorption spectrum of a film, prepared under the same conditions, on glass.

feature is due to charge delocalization over the entire polymer as a result of hybrid electroactivity from both redox-active centers (i.e., conjugated chain and TTF). In polymer **3**, independent redox processes are detected by UV−vis spectroelectrochemistry and supported by computational studies.

Despite the unusual redox behavior of polymers **1** and **4**, we have demonstrated that such materials can still function as organic semiconductors in solar cell devices. Polymer **4** is a low band gap, PTV-based material which is stable under ambient conditions and solution processable. In blends with PCBM, photoluminescence is not significantly affected, providing further evidence that charge transfer does not affect the electronic structure of the main chain. Blends of **4**:PCBM deliver a photocurrent up to 850 nm, which represents the onset of the $\pi-\pi^*$ absorption band of the conjugated PTV chain. Since the electron donating sites within the structure of **4** originate from the TTF units, photoinduced electron transfer must involve the participation of the PTV chain and the TTF species in tandem. Spontaneous charge transfer between the TTFs and C_{60} does not take place, because the HOMO−LUMO difference is significantly large (1.45−1.50 eV). Photoexcitation of the polymer is expected to lead to the quinoidal state depicted in Scheme 2. For each 1,3-dithiole unit fused to the main chain, there is now a formal double bond within the ring. The ionization potential for the TTF unit should be lowered in this structure, since the loss of an electron from the fused dithiole ring will be more favored due to the generation of a 6π aromatic intermediate. It is feasible, therefore, that photoexcitation of the polymer initiates this process and fosters electron transfer from the TTF unit to the fullerene acceptor.

Acknowledgment. P.J.S. would like to thank The Leverhulme Trust (F/00120/U) for funding R.B., and the EPSRC (GR/T28379) for funding A.K. and J.L., and for funding the UK multi-frequency EPR center in Manchester. W.C. thanks the EPSRC and CCLRC for provision of synchrotron diffraction facilities through the UK National Crystallography Service.

Supporting Information Available: Experimental data for the synthesis and characterization of compound **11** and polymers **2**−**4**, MALDI-TOF mass spectrum and ^{1}H NMR spectrum of **4**, crystallographic information file (CIF) and description of crystallographic procedures for compound **8** and diagram depicting the unit cell contents, cyclic voltammogram showing the electrochemical growth of polymer **3**, and additional computational data and related figures. This material is available free of charge via the Internet at http://pubs.acs.org.

References and Notes

(1) Dimitrakopoulos, C. D.; Malenfant, P. R. L. *Adv. Mater*. **2002**, *14*, 99−117.
(2) Sun. Y.; Liu, Y.; Zhu, D. *J. Mater. Chem*. **2005**, *15*, 53−65.
(3) Ling, M. M.; Bao, Z. *Chem. Mater*. **2004**, *16*, 4824−4840.
(4) Tian, H.; Wang, J.; Shi, J.; Yan, D.; Wang, L.; Geng, Y.; Wang, F. *J. Mater. Chem*. **2005**, *15*, 3026−3033.
(5) Kraft, A.; Grimsdale, A. C.; Holmes, A. B. *Angew. Chem., Int. Ed*. **1998**, *37*, 402−428.
(6) Dini, D. *Chem. Mater.* **2005**, *17*, 1933−1945.
(7) Akcelrud, L. *Prog. Polym. Sci.* **2003**, *28*, 875−962.
(8) Mortimer, R. J. *Chem. Soc. Rev.* **1997**, *26*, 147−156.
(9) Gaupp, C. L.; Zong, K.; Schottland, P.; Thompson, B. C.; Thomas, C. A.; Reynolds, J. R. *Macromolecules* **2000**, *33*, 1132−1133.
(10) Cirpan, A.; Argun, A. A.; Grenier, C. R. G.; Reeves, B. D.; Reynolds, J. R. *J. Mater. Chem.* **2003**, *13*, 2422−2428.
(11) Sonmez, G.; Sonmez, H. B.; Shen, C. K. F.; Jost, R. W.; Rubin, Y.; Wudl, F. *Macromolecules* **2005**, *38*, 669−675.
(12) Meng, H.; Wudl, F. *Macromolecules* **2001**, *34*, 1810−1816.
(13) Pomerantz, M.; Gu, X.; Zhang, S. X. *Macromolecules* **2001**, *34*, 1817−1822.
(14) Benincori, T.; Rizzo, S.; Sannicolò, F.; Schiavon, G.; Zecchin, S.; Zotti, G. *Macromolecules* **2004**, *36*, 5114−5118.
(15) Seshadri, V.; Sotzing, G. A. *Chem. Mater*. **2004**, *16*, 5644−5649.
(16) Zaman, M. B.; Perepichka, D. F. *Chem. Commun*. **2005**, 4187−4189.
(17) Sonmez, G.; Shen, C. K. F.; Rubin, Y.; Wudl, F. *Adv. Mater*. **2005**, *17*, 897−900.
(18) Brabec, C. J.; Sariciftci, N. S.; Hummelen, J. C. *Adv. Funct. Mater.* **2001**, *11*, 15−26.
(19) Shaheen, S. E.; Ginley, D. S.; Jabbour, G. E. *MRS Bull.* **2005**, *30*, 10−22.
(20) Segura, J. L.; Martín, N.; Guldi, D. M. *Chem. Soc. Rev.* **2005**, *34*, 31−47.
(21) Le Floch, F.; Ho, H.-A.; Harding-Lepage, P.; Bédard, M.; Neagu-Plesu, R.; Leclerc, M. *Adv. Mater.* **2005**, *17*, 1251−1254.
(22) Martinez-Diaz, M. V.; Esperanza, S.; De la Escosura, A.; Catellani, M.; Yunus, S.; Luzzati, S.; Torres, T. *Tetrahedron Lett.* **2003**, *44*, 8475−8478.
(23) Wolf, M. O. *Adv. Mater.* **2001**, *13*, 545−553.
(24) Ko, H. C.; Park, S.; Paik, W.; Lee, H. *Synth. Met.* **2002**, *132*, 15−20.
(25) Kijima, M.; Setoh, K.; Shirakawa, H. *Chem. Lett.* **2000**, 936−937.
(26) Yamazaki, T.; Murata, Y.; Komatsu, K.; Furukawa, K.; Morita, M.; Maruyama, N.; Yamao, T.; Fujita, S. *Org. Lett.* **2004**, *6*, 4865−4868.
(27) Murata, Y.; Suzuki, M.; Komatsu, K. *Org. Biomol. Chem.* **2003**, *1*, 2624−2625.
(28) Catellani, M.; Luzzati, S.; Lupsac, N. O.; Mendichi, R.; Consonni, R.; Famulari, A.; Meille, S. V.; Giacalone, F.; Segura, J. L.; Martin, N. *J. Mater. Chem.* **2004**, *14*, 67−74.
(29) Iraqi, A.; Crayston, J. A.; Walton, J. C. *J. Mater. Chem.* **1998**, *8*, 31−36.
(30) Bryce, M. R.; Chissel, A. D.; Gopal, J.; Kathirgamanathan, P.; Parker, D. *Synth. Met*. **1991**, *39*, 397−400.
(31) Thobie-Gautier, C.; Gorgues, A.; Jubault, M.; Roncali, J. *Macromolecules* **1993**, *26*, 4094−4099.
(32) Huchet, L.; Akoudad, S.; Levillain, E.; Roncali, J.; Emge, A.; Bäuerle, P. *J. Phys. Chem. B* **1998**, *102*, 7776−7781.
(33) Huchet, L.; Akoudad, S.; Roncali, J. *Adv. Mater*. **1998**, *10*, 541−545.
(34) Skabara, P. J.; Berridge, R.; McInnes, E. J. L.; West, D. P.; Coles, S. J.; Hursthouse, M. B.; Müllen, K. *J. Mater. Chem*. **2004**, *14*, 1964−1969.
(35) Kotani, S.; Shiina, K.; Sonogashira, K. *J. Organomet. Chem*. **1992**, *429*, 403−413.
(36) Renaldo, A.; Labadie, J. W.; Stille, J. K. *Org. Synth.* **1989**, *67*, 86−97.
(37) Skabara, P. J.; Roberts, D. M.; Serebryakov, I. M.; Pozo-Gonzalo, C. *Chem. Commun.* **2000**, 1005−1006.
(38) Saito, G. *Pure Appl. Chem.* **1987**, *59*, 999−1004.
(39) Skabara, P. J.; Serebryakov, I. M.; Roberts, D. M.; Perepichka, I. F.; Coles, S. J.; Hursthouse, M. B. *J. Org. Chem.* **1999**, *64*, 6418−6424.
(40) Skabara, P. J.; Pozo-Gonzalo, C.; Khan, T.; Roberts, D. M.; Light, M. E.; Hursthouse, M. B.; Sariciftci, N. S.; Neugebauer, H.; Cravino, A. *J. Mater. Chem.* **2002**, *12*, 500−510.
(41) Wang, C.; Schindler, J. L.; Kannewurf, C. R.; Kanatzidis, M. G. *Chem. Mater*. **1995**, *7*, 58−68.
(42) Tran-Van, F.; Garreau, S.; Louarn, G.; Froyer, G.; Chevrot, C. *J. Mater. Chem.* **2001**, *11*, 1378−1382.
(43) Khan, T.; McDouall, J. J. W.; McInnes, E. J. L.; Skabara, P. J.; Frère, P.; Coles, S. J.; Hursthouse, M. B. *J. Mater. Chem*. **2003**, *13*, 2490−2498.
(44) Khan, T.; Skabara, P. J.; Frère, P.; Allain, M.; Coles, S. J.; Hursthouse, M. B. *Tetrahedron Lett*. **2004**, *45*, 2535−2539.
(45) Crouch, D. J.; Skabara, P. J.; Heeney, M.; McCulloch, I.; Coles, S. J.; Hursthouse, M. B. *Chem. Commun*. **2005**, 1465−1467.
(46) Crouch, D. J.; Skabara, P. J.; Lohr, J. E.; McDouall, J. J. W.; Heeney, M.; McCulloch, I.; Sparrowe, D.; Shkunov, M.; Coles, S. J.; Horton, P. N.; Husthouse, M. B. *Chem. Mater*. **2005**, *17*, 6567−6578.
(47) Bondi, A. *J. Phys. Chem.* **1964**, *68*, 441−451.
(48) Frère, P.; Skabara, P. J. *Chem. Soc. Rev.* **2005**, *34*, 69−98.
(49) Skabara, P. J.; Berridge, R.; Prescott, K.; Goldenberg, L. M.; Ortí, E.; Viruela, R.; Pou-Amérigo, R.; Batsanov, A. S.; Howard, J. A. K.; Coles, S. J.; Hursthouse, M. B. *J. Mater. Chem.* **2000**, *10*, 2448−2457.
(50) Berridge, R.; Serebryakov, I. M.; Skabara, P. J.; Ortí, E.; Viruela, R.; Pou-Amérigo, R.; Coles S. J.; Hursthouse, M. B. *J. Mater. Chem*. **2004**, *14*, 2822−2830.
(51) Skabara, P. J.; K.; Müllen, K. *Synth. Met.*, **1997**, *84*, 345−346.
(52) Huchet, L.; Akoudad, S.; Roncali, J. *Adv. Mater.* **1998**, *10*, 541−545.
(53) Roncali, J. *Chem. Rev.* **1997**, *97*, 173−205.
(54) Spencer, H. J.; Skabara, P. J.; Giles, M.; McCulloch, I.; Coles, S. J.; Hursthouse, M. B. *J. Mater. Chem.* **2005**, *15*, 4783−4792.

(55) Huchet, L.; Akoudad, S.; Levillain, E.; Roncali, J.; Emge, A.; Bäuerle, P. *J. Phys. Chem. B* **1998**, *102*, 7776−7781.

(56) Torrance, J. B.; Scott, B. A.; Welber, B.; Kaufman, F. B.; Seiden, P. E. *Phys. Rev. B* **1979**, *19*, 730−741.

(57) Kaufman, F. B.; Schroeder, A. H.; Engler, E. M.; Kramer, S. R.; Chambers, J. Q. *J. Am. Chem. Soc.* **1980**, *102*, 483−488.

(58) Khodorkovsky, V.; Shapiro, L.; Krief, P.; Shames, A.; Mabon, G.; Gorgues, A.; Giffard, M. *Chem. Commun.* **2001**, 2736−2737.

(59) Mason, C. R.; Skabara, P. J.; Cupertino, D.; Schofield, J.; Meghdadi, F.; Ebner, B.; Sariciftci, N. S. *J. Mater. Chem.* **2005**, *15*, 1446−1453.

(60) Berridge, R.; Wright, S. P.; Skabara, P. J. Manuscript in preparation.

(61) Cavara, L.; Gerson, F.; Cowan, D. O.; Lerstrup, K. *Helv. Chim. Acta* **1986**, *69*, 141−151.

(62) Frisch, M. J.; Trucks, G. W.; Schlegel, H. B.; Scuseria, G. E.; Robb, M. A.; Cheeseman, J. R.; Montgomery, J. A., Jr.; Vreven, T.; Kudin, K. N.; Burant, J. C.; Millam, J. M.; Iyengar, S. S.; Tomasi, J.; Barone, V.; Mennucci, B.; Cossi, M.; Scalmani, G.; Rega, N.; Petersson, G. A.; Nakatsuji, H.; Hada, M.; Ehara, M.; Toyota, K.; Fukuda, R.; Hasegawa, J.; Ishida, M.; Nakajima, T.; Honda, Y.; Kitao, O.; Nakai, H.; Klene, M.; Li, X.; Knox, J. E.; Hratchian, H. P.; Cross, J. B.; Bakken, V.; Adamo, C.; Jaramillo, J.; Gomperts, R.; Stratmann, R. E.; Yazyev, O.; Austin, A. J.; Cammi, R.; Pomelli, C.; Ochterski, J. W.; Ayala, P. Y.; Morokuma, K.; Voth, G. A.; Salvador, P.; Dannenberg, J. J.; Zakrzewski, V. G.; Dapprich, S.; Daniels, A. D.; Strain, M. C.; Farkas, O.; Malick, D. K.; Rabuck, A. D.; Raghavachari, K.; Foresman, J. B.; Ortiz, J. V.; Cui, Q.; Baboul, A. G.; Clifford, S.; Cioslowski, J.; Stefanov, B. B.; Liu, G.; Liashenko, A.; Piskorz, P.; Komaromi, I.; Martin, R. L.; Fox, D. J.; Keith, T.; Al-Laham, M. A.; Peng, C. Y.; Nanayakkara, A.; Challacombe, M.; Gill, P. M. W.; Johnson, B.; Chen, W.; Wong, M. W.; Gonzalez, C.; Pople, J. A. *Gaussian 03*, revision C.02; Gaussian, Inc.: Wallingford, CT, 2004.

(63) Ono, N.; Okumura, H.; Murashima, T. *Heteroat. Chemistry* **2001**, *12*, 414−417.

(64) Roncali, J.; Jestin, I.; Frère, P.; Levillain, E.; Stievenard, D. *Synth. Met.* **1999**, *101*, 667−670.

(65) Martineau, C.; Blanchard, P.; Rondeau, D.; Delaunay, J.; Roncali, J. *Adv. Mater.* **2002**, *14*, 283−287.

(66) Rondeau, D.; Matrineau, C.; Blanchard, P.; Roncali, J. *J. Mass Spectrom.* **2002**, *37*, 1081−1085.

(67) Xie, H.-Q. C.; Liu, M.; Guo, J. S. *Eur. Polym. J.* **1996**, *32*, 1131−1137.

(68) Osaka, I.; Goto, H.; Itoh, K.; Akagi, K. *Synth. Met.* **2001**, *119*, 541−542.

(69) Jestin, I.; Frère, P.; Levillain, E.; Roncali, J. *Adv. Mater.* **1999**, *11*, 134−138.

(70) Brassett, A. J.; Colaneri, N. F.; Bradley, D. D. C.; Lawrence, R. A.; Friend, R. H.; Murata, H.; Tokito, S.; Tsutsui, T.; Saito, S. *Phys. Rev. B* **1990**, *41*, 10586−10594.

(71) Brabec, C. J.; Sariciftci, N. S.; Hummelen, J. C. *Adv. Funct. Mater.* **2001**, *11*, 15−26.

(72) Apperloo, J. J.; Matrineau, C.; van Hal, P. A.; Roncali, J.; Janssen, R. A. J. *J. Phys. Chem. A* **2002**, *106*, 21−31.

(73) Apperloo, J. J.; Raimundo, J. M.; Frère, P.; Roncali, J.; Janssen, R. A. J. *Chem.—Eur. J.* **2000**, *6*, 1698−1707.

(74) Lane, P. A.; Wei, X.; Vardeny, Z. V. *Phys. Rev. Lett.* **1996**, *77*, 1544−1547.

(75) Henckens, A.; Knipper, M.; Polec, I.; Manca, J.; Lutsen, L.; Vanderzande, D. *Thin Solid Films* **2004**, *451*, 572−579.